JJEE

Volume X | Number X | Month 20XX | Pages XXX-XXX

Jordan Journal of Electrical Engineering

ISSN (print): 2409-9600, ISSN (online): 2409-9619

Homepage: jjee.ttu.edu.jo

Enhancing Solar PV System Performance Through the Optimization of PV Cell Parameters Using the Puzzle Optimization Algorithm

Subhasri Kar[1]*, Sumit Banerjee[2], Chandan Kumar Chanda[3]

[1] Department of Electrical Engineering, Netaji Subhash Engineering College, Kolkata, India
E-mail: subhasri.kar@nsec.ac.in

[2] Department of Electrical Engineering, Dr. B. C. Roy Engineering College, Durgapur, India

[3] Department of Electrical Engineering, Indian Institute of Engineering Science and Technology, Shibpur, India

Received: Dec 23, 2024 *Revised: Apr 17, 2025* *Accepted: Apr 27, 2025* *Available online: May 22, 2025*

***Abstract*—** Accurate estimation of solar photovoltaic (PV) parameters plays a crucial role in achieving optimal performance in PV systems, which is essential for theoretical analysis and real-time applications. This paper introduces the Puzzle Optimization Algorithm (POA) as a novel approach for determining the optimum PV parameters in a PV single-diode model. The primary objective is to show the efficacy of this method by evaluating the root mean square error (RMSE) of the objective function. The investigation involves the analysis of four commercial PV modules, with a comparison of RMSE values against recently published literature. Applying the POA to these PV modules, reveals improved accuracy and minimal error in output current. Moreover, using optimized PV parameters, open-circuit voltage, short-circuit current, and maximum power are determined for all the PV modules in MATLAB and compared with manufacturer data. The obtained results unveil that the percentage relative error in both maximum power and short-circuit current is less than 1% for all of the PV modules. All in all, this investigation establishes the effectiveness of the POA in achieving precise parameter estimation for various PV modules, contributing to improved PV system design and operation.

***Keywords*—** PV module; Optimization; Puzzle optimization algorithm; Performance; Root mean square error.

Nomenclature

K	Boltzmann constant	T_N	Nominal operating temperature
N_s	Number of cells in series	k_i	Temperature coefficient of short circuit current
T	Operating temperature	stc	Standard test condition
q	Electron charge	S	Irradiation in w/m^2 at operating temperature
I_{sdm}	Single diode module output current	S_{stc}	Irradiation in w/m^2 at stc
I_{ph}	Photocurrent	I_{sh}	Current through the shunt resistance
I_s	Reference diode saturation current	I_o	Diode saturation current
V_{sdm}	Single diode module output voltage	V_T	Thermal voltage
R_s	Series resistance	AM	Air mass (average solar spectrum)
R_{sh}	Shunt resistance	P_m	Maximum power
n	Ideality factor of the diode	I_{sc}	Short circuit current
$RMSE_{CAL}$	Calculated RMSE	V_{oc}	Open circuit voltage
V_{mp}	Voltage at maximum power	I_{mp}	Current at maximum power

* Corresponding author

DOI: https://doi.org/10.5455/jjee.204-1734940098

1. INTRODUCTION

The extensive exploitation of fossil fuels results in the growth of fossil fuel depletion, unchecked natural pollution, and volatile energy prices [1]. Solar energy is prominent among other renewable sources such as wind, tide, ocean, geothermal, and biomass due to its ample availability, eco-friendliness, cost-effectiveness, and wide range of applications. PV, which directly converts solar energy into electric energy, is a critical technology in this domain [2]. Within a PV system, arrays of series-parallel connected PV modules serve as the primary energy source. However, the nonlinear behaviors exhibited by PV characteristics pose a significant challenge, prompting researchers to rigorously model these modules for enhanced accuracy [3, 4]. Researchers have explored mathematical approaches to capture the details of PV systems' nonlinear performance in pursuit of precise modeling. The outline of equivalent circuits has proven its worthiness in comprehending module behaviors, and in the field of solar PVs, two distinct types of equivalent circuits have emerged. The single and double-diode equivalent circuit models have acquired substantial attention, primarily through mathematical formulations. The SDM exhibits superior applicability over the DDM, except under low irradiation conditions [4]. For in-depth analysis of current (I) – voltage (V) and power (P) – voltage (V) characteristics, the SDM has demonstrated its effectiveness as a versatile and proven model. This model facilitates the determination of the five essential parameters associated with the SDM equivalent circuit [5]. In practice, these ideas are often tested using experimental setups like the one shown in Fig. 1, which help collect current and voltage characteristics for PV modules.

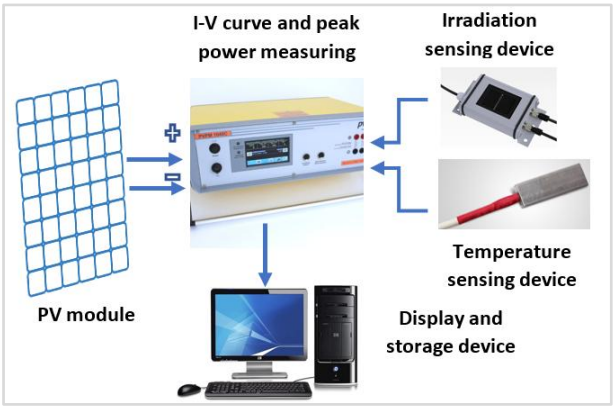

Fig. 1. Experimental arrangement for obtaining the peak power and the current-voltage characteristics.

Five essential parameters are present within the single diode model (SDM): photocurrent, diode saturation current, ideality factor, series and shunt resistance. Accurate determination of these parameters is crucial, and SDM analysis takes care of both precision and simplicity when compared to the double diode model [6]. Assigning precise values to these parameters for an actual solar cell proves to be a challenging task. While analytical approaches offer straightforward solutions, they often require approximations to capture the fundamental nature of the PV cell's diverse characteristics and behaviours [7]. Standard stepwise techniques such as the Newton-Raphson Method (NRM) are favoured to derive accurate PV parameters, overshadowing alternatives such as bisection and false position methods [8]. In [9], a modified NRM addresses the nonlinear transcendental equation within the PV cell. However, this iterative approach encounters limitations due to model constraints, potentially leading to local optima [10]. To deal with errors from repeated trial methods,

metaheuristic algorithms are used to find better solutions for complex problems. Researchers have introduced recent optimization algorithms like the gaining-sharing knowledge-based algorithm (GSK) [11], musical chair algorithm (MCA) [12], modified particle swarm optimization (PSO) [13] etc. Ahmed et al. proposed Particle Swarm Optimization (PSO) and its improved versions to optimize the benefits derived from solar panels. The standard PSO (SPSO) algorithm faces challenges such as low convergence speed, trouble in parameter adjustment, and susceptibility to getting trapped in local maximum power points (LMPPs) during rapid variation in solar irradiance or partial shading conditions (PSCs). A new enhanced MPPT method using a Superior version of the Autonomous Group PSO (EAGPSO) algorithm is suggested in response to these challenges. In [14], the HMSCPSO, Hybrid Multi-Group Stochastic Cooperative PSO algorithm is introduced.

The suggested algorithm incorporates a multi-group cooperation search approach to enhance global search capabilities, with every group employing dissimilar search methods. The first group uses the fundamental way to update speed and position, the second integrates the chaos strategy, and the third utilizes the levy flight approach. The algorithm aims to increase population diversity by fostering group cooperation, reducing the likelihood of converging to local optima. Simultaneously, it encourages specific entities to discover the global optimum, enhancing the correctness of the solution. In [15], an improved Gradient-Based Optimizer (GBO) iteration is presented to estimate unknown parameters in diverse PV models. The enhancement involves integrating the Criss-Cross (CC) algorithm and the Nelder–Mead simplex (NMs) methodology with the GBO to elevate its overall efficacy. Incorporating the CC algorithm maximizes population performance and prevents entrapment in local optima. Despite these advancements, a comprehensive algorithm that accurately addresses the optimization lacks clear information. According to the non-free lunch theorem, each optimization solution has the potential for improvement [16], thereby rendering the search for competitive and efficient metaheuristics for PV parameter estimation an ongoing challenge.

In this study, a novel approach named the POA is introduced to fine-tune parameter values of a PV module, with the core objective of minimizing output current error and thereby enhancing overall PV system performance. The uniqueness of the POA lies in its game-based framework, wherein participants collaboratively solve a puzzle. This game-based strategy offers a unique correlation that distinguishes it from traditional optimization algorithms. The study links puzzle-solving and optimization, demonstrating how the algorithm strategically assembles puzzle pieces at optimal positions, effectively reducing the time required for convergence. The POA unfolds in two main steps: participants work on solving their puzzles while imitating others and offer advice on suitable puzzle pieces to assist those facing difficulties. This study examines four benchmark PV modules—Photo watt PWP201, STP6-120/36, KC200GT, and Shell ST40—to assess the correctness and performance of the POA. It analyzes the root mean square output current error values for five parameters and compares them with results from well-known metaheuristic algorithms. The algorithm is implemented in the four PV modules, and its efficacy is assessed by analyzing the root mean square error (RMSE). The outcomes show that the POA algorithm outperforms others in accuracy, resulting in a highly effective technique for optimizing solar PV parameters. POA algorithm is applied to retrieve PV parameters. The key highlights of this paper include:

- A novel use of the POA algorithm is shown in this paper to determine the best values of the PV parameters of the four PV models, where the POA algorithm suitability compared to other metaheuristic (MH) algorithms is witnessed by the objective function value and rate of convergence.
- The performance of the proposed POA algorithm is evaluated using RMSE.
- The performance of the POA algorithm is assessed through comparison with other MH algorithms, like DE [17], FADE [18], LMSA [19], HFAPS [20], and COA [21].
- The results highlight that the POA algorithm provides the lowest error in RMSE and is superior to other existing literature.

The paper's structure includes several distinct sections. Section 2 overviews the PV module and the mathematical foundation underlying the objective function. Section 3 elaborates on the novel algorithm's working, supplemented by a visual flowchart of its operational process. In Section 4, the findings are discussed and compared. In addition, a comparative study was added to verify the effectiveness of POA. After optimization, the performance parameters are found from MATLAB simulation and compared with the manufacturer data. Finally, Section 5 encapsulates the comprehensive conclusions.

2. MODELING OF THE PV MODULE AND PROBLEM FORMULATION

2.1. Single Diode PV Model

A PV module comprises multiple P-N junction solar cells interconnected in a series configuration. The model's equivalent circuit and performance attributes depend on five crucial parameters. The illustration in Fig. 2 depicts the architecture of a PV cell using a single-diode model with I_{ph} denoting the photocurrent, I_d representing the current flows in the diode, R_s signifying the series of resistance, R_{sh} standing for the module's shunt resistance, I_{sh} indicating the shunt path current and I_{sdm} and V_{sdm} denoting the current and voltage outputs of the SDM model, respectively.

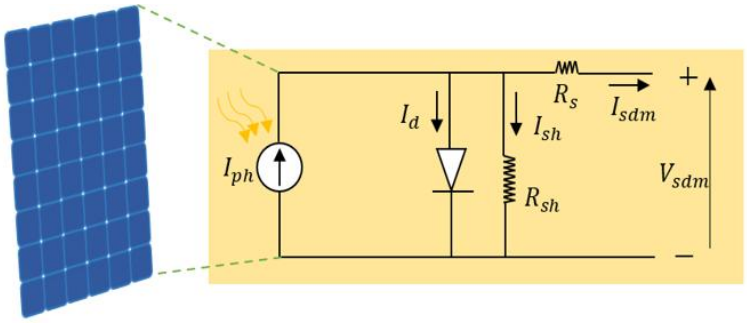

Fig. 2. Electrical equivalent circuit of a single diode PV model.

Shockley diode equation and Kirchhoff's current law give the current equation of the single diode model (SDM) as:

$$I_{sdm} = I_{ph} - I_s\left[exp\left(\frac{V_{sdm}+I_{sdm}R_s}{\frac{nN_sKT}{q}}\right)-1\right]-\left(\frac{V_{sdm}+I_{sdm}R_s}{R_{sh}}\right) \quad (1)$$

where I_s is the diode saturation current, n is the diode ideality factor, K is Boltzmann constant ($1.3806503 \times 10^{-23}$ J/K), q is the electron charge ($1.60217646 \times 10^{-19}$ C), T is temperature and N_s is the number of series-connected cells.

Four PV modules were chosen to assess the POA algorithm's effectiveness, including three polycrystalline modules and one thin-film module. In addition to the conventional crystalline silicon solar cells, the applicability of the current algorithm was extended to the Shell ST40 module, which comprises a monolithic arrangement of series-connected solar cells based on Copper Indium Diselenide (CIS) technology. The electrical attributes of these modules are presented in detail in Table 1.

Table 1. Electrical attributes of the designated four PV modules.

PV module parameter	PV module			
	Photo watt PWP201 [22]	KC200GT [23]	Shell ST40 [24]	STP6-120/36 [25]
I_{sc}	1.03A	8.21 A	2.68	7.33A
V_{oc}	16.778V	32.9 V	23.3	21.24V
I_{mp}	0.89789A	7.61 A	2.41	6.67A
P_m	12W	200W	40	120W
V_{mp}	12.6V	26.3 V	16.6	18V
T	45˚C	25˚C	25˚C	25˚C
N_s	36	54	36	36
S	1000W/m²	1000W/m²	1000W/m²	-

In addition to utilizing optimization techniques for parameter extraction from a PV module, a more comprehensive investigation is necessary to enhance the accuracy and align it closely with the module's actual characteristics curve. The Eqs. (1-6) [26] offer valuable insights for creating a PV Simulink model in MATLAB.

$$I_o = \left(\frac{T}{T_N}\right)^3 * I_s * e^{\left[\left(\frac{1}{T_N}-\frac{1}{T}\right)*q*\frac{Ego}{nK}\right]} \quad (2)$$

Eq. (2) represents the diode saturation current, I_o and it is proportional to cell temperature, T. E_{go} is the bandgap energy of the semiconductor. The light-generated current of the PV module can be expressed as:

$$I_{ph} = [I_{sdm} + \{k_i * (T - T_N)\}] * \frac{S}{S_{stc}} \quad (3)$$

k_i is the temperature coefficient of the short circuit current.

Variations in PV module temperature led to fluctuations in the short circuit current. Each PV module technology possesses its distinct temperature coefficient. Eq. (4) subsequently depicts the current within the shunt resistance branch, as illustrated in Fig. 2. This shunt current is influenced by both the module's series resistance and its shunt resistance. The symbol R_s represents the effective contact resistance resulting from the aggregation of all cells within the module, while R_{sh} denotes the effective leakage resistance originating from the interconnected cells within the module.

$$I_{sh} = \frac{V_{sdm}+I_{sdm}*R_s}{R_{sh}} \quad (4)$$

Eq. (5) presents the reference saturation current of the diode where V_T is the thermal voltage, which depends on the number of cells and the module's operating temperature, as expressed in Eq. (6).

$$I_s = \frac{I_{sc}}{e^{\left[\frac{V_{oc}}{n*V_T}\right]-1}} \quad (5)$$

$$V_T = \frac{N_s KT}{q} \tag{6}$$

The above mathematical formulations from Eqs. (1) to (6) are the basis of mathematical simulation of a PV module from where the $I-V$ and $P-V$ characteristics can be found.

2.2 Objective Function

This paper aims to unearth discrepancies and measure the accuracy between real-world and computational data matches after making improvements. Using the optimized parameters: photocurrent (I_{ph}), diode saturation current (I_s), ideality factor (n), series resistance (R_s), and shunt resistance (R_{sh}), the study scrutinizes the consistency between calculated and measured output currents. This endeavour revolves around minimizing the encountered errors, with the error minimization puzzling problem framed as the objective function shown in Eq. (7). Root mean square error (RMSE), a widely accepted benchmark statistical measure in numerous works [17, 18, 27-33], is the chosen measuring tool to assess this error. Formulated as Eq. (8), RMSE emerges as a pivotal index for quantifying accuracy.

$$f_{sdm}(V_{sdm}, I_{sdm}, D_v) = \left(I_{ph} - I_s\left[exp\left(\frac{V_{sdm}+ I_{sdm}R_s}{\frac{nN_sKT}{q}}\right) - 1\right] - \left(\frac{V_{sdm}+ I_{sdm}R_s}{R_{sh}}\right) - I_{sdm}\right) \tag{7}$$

$$RMSE_{CAL} = \sqrt{\frac{1}{N}\sum_{i=1}^{N} f_{sdm}(V_{sdmi}, I_{sdmi}, D_v)^2} \tag{8}$$

Where: $[D_v] = [I_{ph}, I_o, n, R_s, R_{sh}]$ is the decision variable, N = The number of data taken for all parameter, V_{sdmi} is the ith estimated value for the voltage, I_{sdmi} is the ith estimated value for the current.

Hence, it can be summarised as a set of the following objectives:

i. To find $[D_v]$ which accurately describes the model parameter for the actual module output.
ii. To find $f_{sdm}(V_{sdm}, I_{sdm}, D_v)$ which can represent the error compared to the experimental dataset.
iii. To find $RMSE_{CAL}$ which is statistically able to judge the model parameter.

3. OVERVIEW OF THE POA

This section introduces a novel algorithm named the POA, employing a puzzle game-based approach to ascertain the optimal solar PV module parameters that minimize the root mean square error. This algorithm draws inspiration from the strategic tactics used to triumph in puzzle-solving scenarios, positioning it within the family of game-based algorithms. Much like puzzle games such as Sudoku or Candy Crush, the arrangement of boxes or parameters significantly influences the speed of achieving success. The outcome of such games hinges upon the positions and values of these boxes, akin to how the objective function embodies the game results in engineering problems. In the context of a PV plant, these boxes correspond to the parameters that need optimization. In puzzle games, players are tasked with altering the positions of these boxes to achieve victory. Likewise, in the POA, the algorithm initializes parameters randomly within their specified operational bounds. Each solution corresponds to a distinct population, dictating the values and positions of the variables. The algorithm starts by randomly initializing a population of possible solutions, each expressing a unique configuration of PV module parameters. These solutions, or 'puzzle pieces,' are estimated

based on their suitability, which is figured out by how well they minimize the current output's root mean square error (RMSE). Like puzzle games, where players manipulate pieces to fit correctly, the POA iterates by adjusting and reordering parameters to optimize the overall system performance. The algorithm progressively refines the solution, employing strategies such as crossover, mutation, or other heuristic methods, ultimately converging toward the optimal configuration for maximum energy output. Beyond its conceptual foundation, POA is a practical optimization tool for complex, nonlinear problems such as solar PV system parameter tuning. The goal in this context is to enhance system performance by minimizing output current error through fine-tuning parameters like photocurrent (I_{ph}), diode saturation current (I_s), series resistance (R_s), shunt resistance (R_{sh}), diode ideality factor (n)—an inherently difficult task due to fluctuating weather conditions and nonlinear system behavior. To tackle this, POA incorporates a set of core mechanics: search space exploration to identify optimal regions, fitness evaluation based on output accuracy, stochastic processes to maintain diversity and avoid premature convergence, iterative improvements for solution refinement, and global search strategies to escape local optima. These techniques enable POA to navigate the optimization landscape effectively, making it a robust approach for real-world PV system challenges. The POA can be better understood through a simple, step-by-step visual. Imagine each PV parameter (like I_{ph}, I_s, R_s, R_{sh}, and n) as a puzzle piece. At first, the pieces are randomly scattered, showing the starting point of the algorithm. Different solutions try to fit the pieces together as the process begins—some fit well, others don't—just like POA testing various combinations to reduce error. Over time, solutions learn from each other, sharing helpful changes, which speeds up the process. Gradually, the puzzle comes together with fewer gaps, symbolizing how the error gets smaller. In the end, the completed puzzle shows the optimized parameters, proving how POA can find the best solution faster and more accurately than other methods. This visual makes it easier to understand how POA works step by step.

3.1. Mathematics of POA

The POA – flow chart of which is depicted on Fig. 3 - is a population-based method inspired by puzzle games. In POA, each solution is treated as a puzzle, where the puzzle pieces represent the problem's variables. The more wisely the pieces fit, the higher the score, which is determined by the objective function value. The algorithm uses guidance from other members of the population, especially the best solution, to improve its results. In the proposed POA, which is a population-based algorithm, each population member is a feasible candidate to the optimization problem of variables' values. The population in the POA algorithm is mathematically characterized in Eq. (9).

$$V = \begin{bmatrix} V_1 \\ \vdots \\ V_i \\ \vdots \\ V_N \end{bmatrix}_{N\times M} = \begin{bmatrix} v_{11} & \cdots & v_{1d} & \cdots & v_{1m} \\ \vdots & \ddots & \vdots & \iddots & \vdots \\ v_{i1} & \cdots & v_{id} & \cdots & v_{im} \\ \vdots & \iddots & \vdots & \ddots & \vdots \\ v_{N1} & \cdots & v_{Nd} & \cdots & v_{Nm} \end{bmatrix}_{N\times m} \tag{9}$$

where: V is the population of the puzzle, V_i is the puzzle in the ith number, N is the population number contained in the puzzle, m denotes the total count of variables, v_{id} denotes the value of the dth variable in ith puzzle.

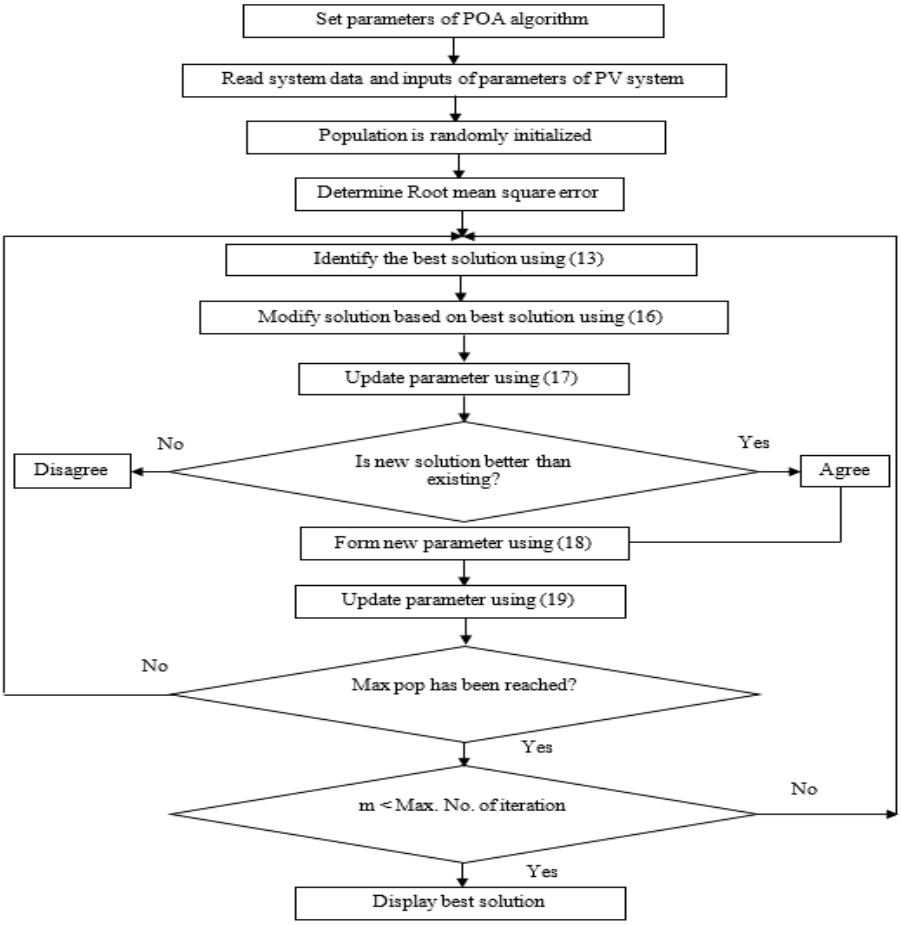

Fig. 3. Flowchart of the presented POA.

3.1.1. Identification of best member:

In the population matrix, each member offers a solution to the problem. Therefore, the objective function value is found. Hence, the number of populations will be the number of objective functions. The objective function (F) is written as Eq. (10).

$$F = \begin{bmatrix} f_1 \\ \vdots \\ f_i \\ \vdots \\ f_N \end{bmatrix}_{N\times 1} \tag{10}$$

Where f_i is the function value in the ith puzzle. Based on the values in the F matrix, the best members are selected by taking the minimum function value.

The connection between the objective function and POA can be viewed as simpler to offer a more precise understanding. The POA uses the objective function to evaluate how well a solution—an arrangement of parameters—performs. The objective function is a mathematical expression that needs to be minimized or maximized, depending on the goal. For instance, in a PV system, the objective might be to reduce the root mean square error to achieve the most efficient setup. Like solving a puzzle game, POA tries different values to see which one works best to find the optimal configuration. It tests different combinations and uses the objective function to score each one, ultimately seeking the arrangement that yields the lowest error and, thus, the best performance. This algorithm unfolds across a series of steps, outlined as follows.

3.2. Initialization

Initial parameter values have been set within their respective minimum and maximum operational limits, following a practice like other optimization algorithms, as indicated by Eq. (11). The size of the population is denoted as 'row', while the count of variables is referred to as 'column'. Once the initialization matrix is established, the determination of the objective function comes into play, with its computation being contingent upon the variable values.

$$Para = Para_{min} + rand * (Para_{max} - Para_{min}) \tag{11}$$

The objective function in Eq. (12) is established according to the parameter value derived from the initialized set. Identifying the best value hinges on evaluating the objective or fitness function. In the context of a minimization problem, the 'Best Member' in Eq. (13) within the pool refers to the value that attains the minimum.

$$Obj.Functn. = f(Para) \tag{12}$$

$$Best\ Member = Min.(Obj.Functn.) \tag{13}$$

3.3. Phase of the Best Member

The initial phase entails the revision of every population member, guided by input from fellow members. Following the identification of the top-performing member, a fresh solution emerges by drawing inspiration from this standout individual. The best member imparts their insights to the rest, facilitating the creation of a novel solution. Initially, a parameter is calculated using Eqs. (14) to (17) by comparing the objective functions of the best member and a specific solution. Upon multiplying this parameter by a random value, a new solution comes into being, which is subsequently incorporated into the existing solution value.

$$Best\ member = Para_i \qquad i \in \{1,2,3 \dots \dots N\} \tag{14}$$

$$I = round(1 + rand) \tag{15}$$

$$Mm_{i,d} = \begin{cases} (Best\ Mem_{i,d} - I \times Para_{i,d}), & Obj.Fuctn._g \leq Obj.Fuctn._i \\ (Para_{i,d} - I \times Best\ Mem_{i,d}), & else \end{cases} \tag{16}$$

$$Para_i^{new} = Para_i + rand \times Mm_i \tag{17}$$

3.4. Phase of Interaction Between Particles

During this stage, each solution undergoes an update through mutual interactions. As the wisdom of the best member permeates every solution, a subsequent cycle of mutual interactions refines these solutions once more, as outlined in Eq. (18).

$$Para_{i,d_j}^{new} = Para_{h,d_j} \qquad \begin{Bmatrix} h \in 1,2, \dots \dots \dots \dots \dots \dots Pop\_size \\ j \in 1,2, \dots \dots suggested\ puzzles \\ d \in 1,2, \dots \dots \dots no\_of\_variables \end{Bmatrix} \tag{18}$$

Upon attaining a fresh solution, the objective function is computed. A comparison is made between the newly acquired and obtained fitness values during initialization. The solution associated with the minimum objective function value is reserved for the subsequent iteration. Subsequently, a new solution is chosen for the ensuing iteration employing Eq. (19).

$$Para_i = \begin{cases} Para_i^{new}, obj.funtn_i^{new} \langle obj.functn._i \\ Para_i \quad else \end{cases} \tag{19}$$

4. RESULTS ANALYSIS

4.1. Optimization

In this research, the POA was explained using a flowchart illustrated in Fig. 3, and its implementation was realized in MATLAB 2015(b). The proposed POA methodology has been executed across four distinct PV modules to determine optimal parameter values that minimize the error in the current output. Consequently, the assessment of root mean square error succeeded. This comprehensive investigation contained three separate polycrystalline PV modules, namely Photo watt PWP201, STP6-120/36, Kyocera KC200GT and one thin-film module, the Shell ST40. The proposed algorithm's efficacy has been confirmed by verifying all relevant parameters, encompassing photocurrent, diode saturation current, series resistance, shunt resistance, and ideality factor. The POA is applied to four different types of solar PV modules to find the best settings to minimize errors in the current output. The results have been verified by comparing them with the existing literature, ensuring the accuracy of the POA. Table 1 has assembled the particulars of the aforementioned PV modules, and the ensuing sections explore distinct case studies.

4.1.1. Case Study I: Photo watt PWP201 PV Module

Utilizing the proposed algorithm, the optimal parameters for a 12-watt Photowatt-PWP201 PV module have been successfully determined. The root mean square error (RMSE) associated with these parameters has been compared against RMSE values obtained from other established optimization algorithms. Table 2 presents a comprehensive overview of the five parameters and the associated RMSE values derived from the POA algorithm, which are then contrasted with those achieved through prior optimization algorithms. Table 2 shows that the root mean square error (RMSE) attained through SA [39] surpasses the results from other reported methods, although the proposed POA algorithm stands as an exception. Notably, the proposed POA algorithm exhibits the highest accuracy, yielding an impressive RMSE of 1.85E-04. This level of precision outperforms various alternative algorithms, including DE, ISCE, EHA-NMS, Rcr-IJADE, ABC-TRR, TLABC, MPCOA, FPA, ABC-DE, Newton, GAMNU, GACCC, SA, FADE, LMSA, among others. The convergence behavior of the objective function (output current error) over iterations is illustrated in Fig. 4(a), while Fig. 4(b) depicts the relationship between RMSE and iteration for the PWP201 PV module.

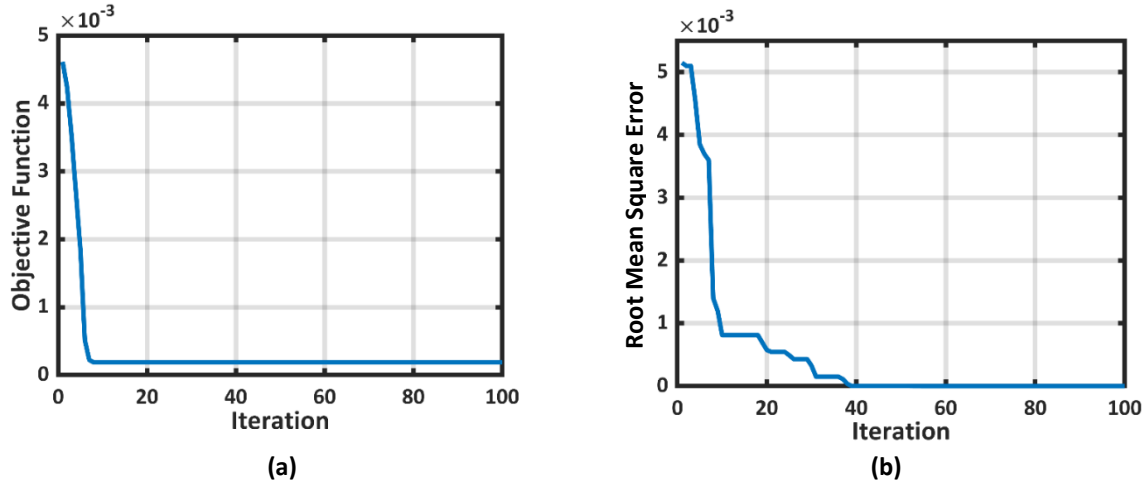

Fig. 4. The PWP201 module: a) variation of the objective function versus iteration; b) the relationship between RMSE and iteration.

Table 2. Parameter retrieval from the Photo watt-PWP 201 module using the proposed POA, alongside alternative methods and RMSE comparison.

Year of report	Methodology	I_{ph}	I_s	R_s	R_{sh}	n	RMSE
Current	POA (proposed)	1.04000	2.00000E-07	1.25000	22.97000	1.30000	1.857100E-04
2019	DE [17]	1.03353	2.12479E-06	0.03471	19.37196	1.30017	2.422747E−03
2018	ISCE [27]	1.03051	3.48226E-06	0.03337	27.27729	1.35119	2.425075E−03
2016	EHA-NMS [28]	1.03051	3.48226E-06	0.03337	27.27728	1.35119	2.425075E−03
2013	Rcr-IJADE [29]	1.03051	3.48226E-06	0.03337	27.27728	1.35119	2.425075E−03
2018	ABC-TRR [30]	1.03051	3.48226E-06	0.03337	27.27728	1.35119	2.425000E−03
2018	TLABC [31]	1.03056	3.47150E-06	0.03338	27.02599	1.35087	2.425070E−03
2014	MPCOA [32]	1.03188	3.37370E-06	0.03342	23.60258	1.34740	2.425100E−03
2015	FPA [33]	1.03209	3.04754E-06	0.03382	22.53811	1.33698	2.742500E−03
2022	FADE [18]	1.03051	3.48226E-06	1.20127	27.27728	1.35100	2.425070E-03
2013	ABC-DE [34]	1.03180	3.27740E-06	0.03351	23.47915	1.34430	3.885500E−03
1986	Newton [35]	1.03180	3.28760E-06	0.03349	15.26250	1.34583	5.601000E−01
2022	[36]	1.03345	2.94840E-06	1.22176	19.90390	1.33392	2.164000E-03
2021	GAMNU [37]	1.03077	3.01623E-06	1.21912	25.17430	1.33604	2.382420E-03
2017	GACCC [38]	1.03051	3.48226E-06	1.20127	27.27738	1.35119	2.425000E-03
2012	SA [39]	1.03310	3.66420E-06	1.19890	23.14815	1.51720	1.700000E-03
2023	LMSA [19]	1.03051	3.47971E-06	1.20149	981.98232	1.35100	2.425125E-03

Beyond the diverse array of optimization algorithms and the assessment of PV parameter extraction, validating accuracy through simulation outcomes holds pivotal significance [40]. Within this study, not only were the optimized parameters derived via the POA algorithm verified, but they were also subjected to mathematical simulations for precision assessment. The POA algorithm to address the optimization objective, the achieved RMSE, was notably lower than the values reported in the existing literature.

4.1.2. Case Study II: STP6-120/36 PV module

Another PV module, the STP6-120/36, with a power output of 120 Watts and operating at 25°C, has also undergone parameter optimization using the proposed algorithm. The RMSE associated with these optimized parameters has been juxtaposed against RMSE values obtained from other recognized optimization algorithms. Detailed in Table 3, are the five parameters governing the Single Diode Model (SDM) of the STP6-120/36 module, along with

the corresponding RMSE values derived from the proposed POA, have been meticulously compared against alternative algorithms.

Table 3. Comparative analysis of parameters in single diode model and RMSE for the STP6-120/36 module in contrast to established algorithms.

Year of report	Method	I_{ph}	I_s	R_s	R_{sh}	n	RMSE
Current	Proposed	7.471500	1.00000E-06	0.005000	9.9000	1.27050996	2.72000E-07
2019	DE [17]	7.483000	0.88680E-06	0.005382	10.5309	1.18720000	1.40910E-02
2022	FADE [18]	7.472530	2.33499E-06	0.004590	22.2200	1.27265000	1.66006E-02
2016	[41]	7.483800	1.20000E-06	0.004900	9.7450	1.20720000	1.78790E-02
2018	ISCE [27]	7.472530	2.33450E-06	0.004595	22.2199000	1.26010348	1.66006E−02

Derived from experimental data, the root mean square error (RMSE) is determined to be 0.014091 [17], reflecting a lower value than that achieved by other established optimization algorithms, except for the POA approach. Remarkably, the proposed algorithm attains an impressively very small RMSE of 2.72E-07, significantly outperforming the figures documented in the current literature.

The convergence dynamics of the objective function (output current error) across iterations are illustrated in Fig. 5(a), while Fig. 5(b) illustrates the relationship between RMSE and the number of iterations for the single diode model of the STP6-120/36 PV module.

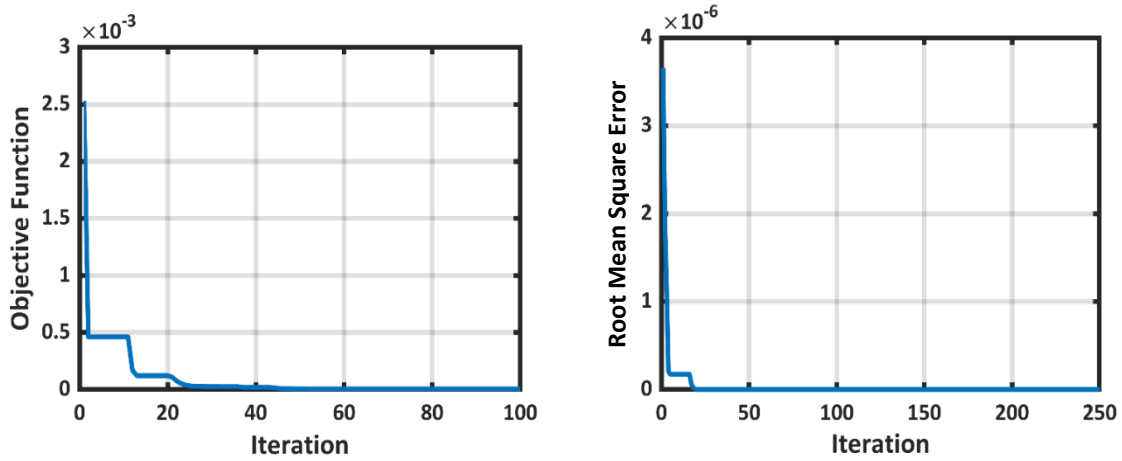

Fig. 5. The STP6-120/36 module: a) convergence of the objective function over iterations; b) the relationship between RMSE and iteration.

4.1.3. Case Study III: Kyocera KC200GT PV module

The third case study involves the Kyocera KC200GT module of 200 Watts, wherein the proposed algorithm was employed and subsequently validated against existing literature. All five parameters have been meticulously presented, accompanied by their corresponding RMSE values.

In a related study, [42] reported an RMSE value of 0.01821364, outperforming [36], [20], and [21]. However, the proposed POA method holds an even more significant advantage among the five, as evidenced by Table 4. Following applying the POA to the single diode

model (SDM) of the KC200GT module, an unprecedented level of efficacy was observed, attaining an RMSE value of 0.012124, as highlighted in Table 4.

Fig. 6 (a) exhibits the characteristics between the objective function and the number of iterations. RMSE characteristics with the number of iterations have been revealed in Fig. 6 (b).

Table 4. Comparative evaluation of parameter optimization for the Kyocera KC200GT PV module, along with the corresponding RMSE, compared to established algorithms.

Year of report	Method	I_{ph}	I_s	R_s	R_{sh}	n	RMSE
Current	Proposed POA	8.25000000	5.0E-10	0.24400000	779.00000	1.299886	0.012124
2022	[36]	-	-	-	-	-	0.271894
2021	WHHO [42]	8.21860582	1.43601E-09	0.24093983	774.212315	1.05528589	0.01821364
2018	HFAPS [20]	8.19924700	1.54161E-07	0.23955200	1448.259000	1.434220	0.04986300
2020	COA[21]	4.66251942	8.71739E-07	0.15231283	2000.000000	1.000000	0.02844810

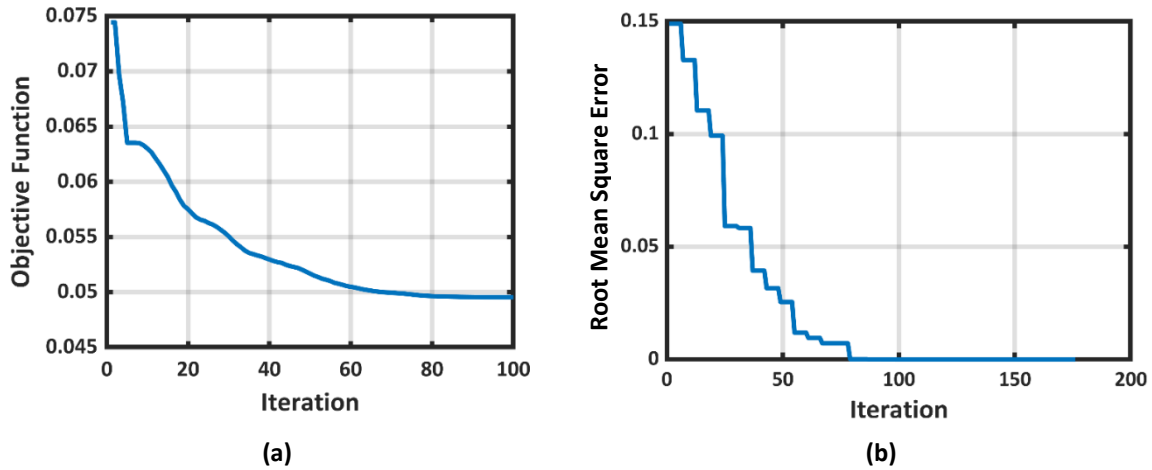

Fig. 6. The KC200GT module: a) convergence of objective function over iterations; b) relationship between RMSE and iteration.

4.1.4. Case Study IV: Shell ST40

Expanding beyond crystalline PV modules, the evaluation now extends to the Shell ST40, a thin-film module with a capacity of 40 Watts and composed of 36 series-connected PV cells. This step aims to reaffirm the accuracy of PV parameters recognized through the POA algorithm. The application of POA to this module seeks to uncover the minimal value of the output current error. The optimal parameters deduced from the POA are then pitted against the findings from [40] and [21]. Upon parameter extraction via the POA, the RMSE value is astonishingly tiny, at 9.93E-13. Table 5 compares various PV parameters derived from the POA, SCT and COA methods. Furthermore, the convergence dynamics of the objective function versus iteration are visualized in Fig. 7. Finally, a concise comparative analysis of POA with other metaheuristic (MH) algorithms is presented herewith.

4.1.5. Comparative Analysis

This section presents the proposed POA, which undergoes rigorous statistical testing through a series of distinct runs (30 for each case/algorithm) to obtain the optimum value of solar parameters. The average rankings for the proposed algorithms across all three solar PV cell/module problems (Photo watt PWP201, STP6-120/36, and Kyocera KC200GT) are

presented in Tables 2, 3 and 4. The outcomes prove the superiority of the POA algorithm over other MH algorithms in addressing all three solar PV cell/module problems. The comparison of the proposed algorithm with different MH algorithms is outlined in Tables 2, 3 and 4. Overall, POA performs better than other algorithms across all three crystalline solar PV cells/modules. Moreover, after crystalline PV modules, a thin film Shell ST40 is considered to showcase the POA algorithm's effectiveness further.

Table 5. Comparison of parameters for the Shell ST40 module with SCT [40] and COA [21].

Estimated variable	By POA	By SCT	By COA
R_s [Ω]	1.2000	1.5362	0.5000000
R_{sh} [Ω]	359.82280	355.03	400.00000
n (dimensionless)	1.45	1.13	2.2884533
I_{ph} [A]	2.690	2.6915	2.6638928
I_s [A]	1.5E-08	1.3E-08	0.5E-08
RMSE	9.93E-13	-	4.71343E-02

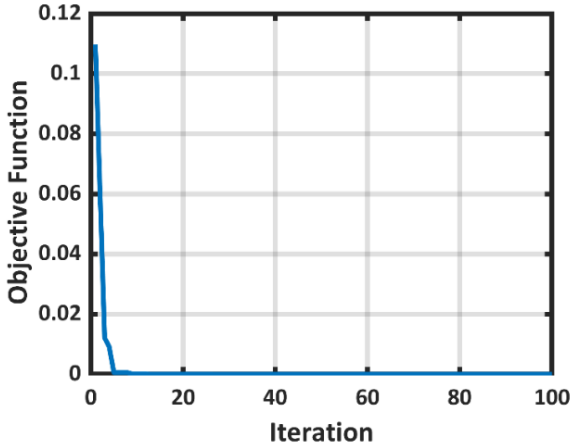

Fig. 7. Convergence of the objective function over iterations for the Shell ST40 module.

Table 5 represents the estimated variables by POA with the parameters obtained by the SCT and COA methods. Also, the RMSE value found from POA for this thin film module is very low, and the convergence plot is shown in Fig. 7. In summary, in the POA versus MH algorithms comparison, the POA algorithm consistently achieves lower RMSE value in all the above solar PV cell/module problems. These results demonstrate the POA algorithm's superior performance to existing MH methods in resolving PV cell/module problems.

4.2. Simulation Result Analysis

The accurate value of PV parameters is necessary to simulate PV modules to achieve the exact P-V and I-V characteristics [26]. The manufacturer datasheet (reference datasheet) does not clearly reveal the required parameter value. POA optimization technique helps to solve this issue.

To further verify the POA's efficacy over the PV parameter estimation, the optimized parameters have been fully utilized to simulate the performance parameters of all the PV modules. Ultimately, open circuit voltage, short circuit current, maximum power, voltage and current at maximum power are found and compared with their reference module data. Comparing with the reference data, it is observed that the overall percentage relative error

(RE) for all the modules in maximum power and short circuit current is below 1%. Percentage RE in open circuit voltage for PWP201, KC200GT PV, Shell ST40 and STP6-120/36 module is 0.1311, 0.3040, 2.1459, and 2.0716, respectively.

The performance parameters found from the simulation are very close to the reference module data. Tables 6-9 compare PV performance parameters for all four modules.

Table 6. Comparison of performance parameters after POA optimization in PWP201module.

Parameter	Reference	Simulated result after optimization	AE	RE	% RE
P_{MPP} [W]	12	11.90	0.10	0.008333	0.8333
V_{MPP} [V]	12.6	12.8	-0.2	0.015873	1.5873
I_{MPP} [A]	0.89789	0.930	0.0321	0.035762	3.5762
I_{SC} [A]	1.03	1.028	0.002	0.0019417	0.1942
V_{OC} [V]	16.778	16.8	-0.022	0.00131124	0.1311

Table 7. Comparison of PV parameters after POA optimization in KC200GT PV module.

Parameter	Reference	Simulated result after optimization	AE	RE	% RE
P_{MPP} [W]	200	199.7	0.3	0.001500	0.1500
V_{MPP} [V]	26.3	26.4	-0.1	0.003802	0.3800
I_{MPP} [A]	7.61	7.563	0.047	0.006176	0.6176
I_{SC} [A]	8.21	8.207	0.003	0.0003654	0.0365
V_{OC} [V]	32.9	32.8	0.1	0.0030395	0.3040

Table 8. Comparison of PV parameters after POA optimization in Shell ST40 PV module.

Parameter	Reference	Simulated result after optimization	AE	RE	% RE
P_{MPP} [W]	40	39.94	0.06	0.0015	0. 15
V_{MPP} [V]	16.6	16.60	0	0	0
I_{MPP} [A]	2.41	2.406	0.004	0.0016597	0.16597
I_{SC} [A]	2.68	2.671	0.009	0.0033582	0.3358
V_{OC} [V]	23.3	22.8	0.5	0.0214592	2.1459

Table 9. Comparison of PV parameters after POA optimization in STP6-120/36 module.

Parameter	Reference	Simulated result after optimization	AE	RE	% RE
P_{MPP} [W]	120	119.400	0.6	0.005	0.5
V_{MPP} [V]	18	17.600	0.4	0.022222	2.2222
I_{MPP} [A]	6.67	6.783	-0.113	0.016942	1.6942
I_{SC} [A]	7.33	7.330	0	0	0
V_{OC} [V]	21.24	20.800	0.440	0.0207156	2.0716

5. CONCLUSIONS

This study explores the practical implementation of the POA for PV parameter extraction, focusing on four prominent commercial PV modules as benchmarks. Specifically, the assessment encompasses the Photowatt-PWP201, STP6-120/36, and Kyocera KC200GT polycrystalline PV modules, chosen to validate the optimized parameters and their corresponding output current error (RMSE). Beyond crystalline modules, the thin-film Shell

ST40 module was also studied to compare various PV parameters with established literature. The RMSE values, produced by the POA application, on both crystalline and thin-film PV modules, show significantly lower output current errors than other established optimization algorithms. This substantiates the superior accuracy of POA in identifying optimal PV parameters within the framework of a single-diode PV module.

On top of that, considering the optimized parameter, all the modules' performance characteristics were observed in the MATLAB simulation to show the further efficacy of POA. A comparison of all performance parameters indicates a good alignment between simulated values and manufacturer data. Consequently, the POA is an effective tool for determining the optimal PV parameters of a PV module. Its application supports precise modeling, facilitating the effective monitoring of robust PV systems. In future work, the POA could be extended to other PV module types - like multi-junction solar cells, organic solar cells, perovskite solar cells, etc. - integrated with real-time data for performance optimization, and combined with machine learning or other advanced techniques for improved accuracy. The POA can be modified for real-time solar power plants by incorporating dynamic reconfiguration techniques to minimize shading effects and mismatch losses to maximize power output. Additionally, considering module ageing and degradation, the algorithm's computational efficiency could be enhanced for large-scale applications and long-term performance predictions could be explored. Future research could also investigate multi-objective optimization frameworks to address cost, reliability, and environmental factors in PV systems.

REFERENCES

[1] B. Sai, S. Khadtare, D. Chatterjee, "A dummy peak elimination based MPPT technique for PV generation under partial shading condition," *IET Renewable Power Generation*, vol. 15, pp. 2438-2451, 2021, doi: 10.1049/rpg2.12175.

[2] S. Li, W. Gong, Q. Gu, "A comprehensive survey on meta-heuristic algorithms for parameter extraction of photovoltaic models," *Renewable and Sustainable Energy Reviews*, vol. 141, pp. 110828, 2021, doi: 10.1016/j.rser.2021.110828.

[3] D. Oliva, M. Aziz, A. Hassanien, "Parameter estimation of photovoltaic cells using an improved chaotic whale optimization algorithm," *Applied Energy*, vol. 200, pp. 141-154, 2017, doi: 10.1016/j.apenergy.2017.05.029.

[4] S. Bana, R. Saini, "A mathematical modelling framework to evaluate the performance of single diode and double diode-based SPV systems," *Energy Reports*, vol. 2, pp. 171–187, 2016, doi: 10.1016/j.egyr.2016.06.004.

[5] N. Yıldıran, E. Tacer, "Identification of photovoltaic cell single diode discrete model parameters based on datasheet values," *Solar Energy*, vol. 127, pp. 175-183, 2016, doi: 10.1016/j.solener.2016.01.024.

[6] H. Mehta, H. Warke, K. Kukadiya, A. Panchal, "Accurate expressions for single-diode-model solar cell parameterization," *IEEE Journal of Photovoltaics*, vol. 9, pp. 1-8, 2019, doi: 10.1109/JPHOTOV.2019.2896264.

[7] J. Cubas, S. Pindado, M. Victoria, "On the analytical approach for modelling photovoltaic systems behaviour," *Journal of Power Sources*, vol. 247, pp. 467-474, 2014, doi: 10.1016/j.jpowsour.2013.09.008.

[8] L. Mathew, A. Panchal, "A complete numerical investigation on implicit and explicit PV single-diode-models using I- and V-approaches," *IEEE Journal of Photovoltaics, vol.* 11, pp. 827-837, 2021, doi: 10.1109/jphotov.2021.3067442.

[9] M. Rasheed, S. Shihab, "Modelling and parameter extraction of PV cell using single-diode models," *Advanced Energy Conversion Materials*, vol. 1, no.2, pp. 96–104, 2020, doi: 10.37256/aecm.122020550.

[10] D. Oliva, E. Cuevas, G. Pajares, "Parameter identification of solar cells using artificial bee colony optimization," *Energy,* vol. 72, pp. 93-102, 2014, doi: 10.1016/j.energy.2014.05.011.

[11] G. Xiong, L. Li, A. Mohamed, X. Yuan, J. Zhang, "A new method for parameter extraction of solar photovoltaic models using gaining–sharing knowledge-based algorithm," *Energy Reports*, vol. 7, pp. 3286-3301, 2021, doi: 10.1016/j.egyr.2021.05.030.

[12] A. Eltamaly, "Musical chairs algorithm for parameters estimation of PV cells," *Solar Energy*, vol. 241, pp. 601-620, 2022, doi: 10.1016/j.solener.2022.06.043.

[13] A. Refaat, A. Khalifa, M. Elsakka, Y. Elhenawy, A. Kalas, M. Elfar, "A novel metaheuristic MPPT technique based on enhanced autonomous group particle swarm optimization algorithm to track the GMPP under partial shading conditions - experimental validation," *Energy Conversion and Management*, vol. 287, no. 1, pp. 117124, 2023, doi: 10.1016/j.enconman.2023.117124.

[14] Y. Lu, S. Liang, H. Ouyang, S. Li, G. Wang, "Hybrid multi-group stochastic cooperative particle swarm optimization algorithm and its application to the photovoltaic parameter identification problem," *Energy Reports*, vol. 9, pp. 4654-4681, 2023, doi: org/10.1016/j.egyr.2023.03.105.

[15] M. Premkumar, P. Jangir, C. Ramakrishnan, C. Kumar, R. Sowmya, S. Deb, N. Kumar, "An enhanced Gradient-based optimizer for parameter estimation of various solar photovoltaic models," *Energy Reports*, vol. 8, pp. 15249-15285, 2022, doi: 10.1016/j.egyr.2022.11.092.

[16] D. Wolpert, W. Macready, "No free lunch theorems for optimization," *IEEE Transactions on Evolutionary Computation, vol.* 1, pp. 67-82, 1997, doi: 10.1109/4235.585893.

[17] V. Chin, Z. Salam, "A new three-point-based approach for the parameter extraction of photovoltaic cells," *Applied Energy*, vol. 237, no. 1, pp. 519-533, 2019, doi: 10.1016/j.apenergy.2019.01.009.

[18] J. Dang, G. Wang, C. Xia, R. Jia, P. Li, "Research on the parameter identification of PV module based on fuzzy adaptive differential evolution algorithm," *Energy Reports*, vol. 8, pp. 12081-12091, 2022, doi: 10.1016/j.egyr.2022.09.057.

[19] F. Dkhichi, "Parameter extraction of photovoltaic module model by using levenberg-marquardt algorithm based on simulated annealing method," *Journal of Computational Electronics*, vol. 22, no. 4, pp. 1128-1139, 2023, doi: 10.1007/s10825-023-02058-0.

[20] A. Mohammadbeigi, A. Maroosi, "Parameter identification for solar cells and module using a hybrid firefly and pattern search algorithms," *Solar Energy*, vol. 171, 2018, doi: 10.1016/j.solener.2018.06.092.

[21] A. Diab, H. Sultan, T. Do, O. Kamel, M. Mossa, "Coyote optimization algorithm for parameters estimation of various models of solar cells and PV modules," *IEEE Access*, vol. 8, pp. 111102-111140, 2020, doi: 10.1109/ACCESS.2020.3000770.

[22] A. Tayyan, "An approach to extract the parameters of solar cells from their illuminated I-V curves using the Lambert W function," *Turkish Journal of Physics,* vol. 39, pp. 1-15, 2015, doi: 10.3906/fiz-1309-7.

[23] *High efficiency multicrystal photovoltaic module*, https://www.energymatters.com.au/images/kyocera/KC200GT.pdf.

[24] *Shell Solar Product Information Sheet*, https://reenergyhub.com/files/hersteller/Shell_Solar/pdf/Shell_Solar_ST40_EN.pdf.

[25] *Solar Schutten*, www.Specification Solar Panel.xlsx.

[26] S. Kar, S. Banerjee, C. Chanda, "Stepwise modelling and analysis of a PV module in Matlab Simulink," *International Conference on Intelligent Technologies (CONIT),"* 2021, doi: 10.1109/CONIT51480.2021.9498343.

[27] X. Gao, Y. Cui, J. Hu, G. Xu, Z. Wang, J. Qu, H. Wang, "Parameter extraction of solar cell models using improved shuffled complex evolution algorithm," *Energy Conversion and Management*, vol. 157, pp. 460-479, 2018, doi: 10.1016/j.enconman.2017.12.033.

[28] Z. Chen, L. Wu, P. Lin, Y. Wu, S. Cheng, "Parameters identification of photovoltaic models using hybrid adaptive Nelder-Mead simplex algorithm based on eagle strategy," *Applied Energy*, vol. 182, pp. 47-57, 2016, doi: 10.1016/j.apenergy.2016.08.083.

[29] G. Wenyin, Z. Cai, "Parameter extraction of solar cell models using repaired adaptive differential evolution," *Solar Energy*, vol. 94, pp. 209-220, 2013, doi: 10.1016/j.solener.2013.05.007.

[30] L. Wu, Z. Chen, C. Long, S. Cheng, P. Lin, Y. Chen, H. Chen, "Parameter extraction of photovoltaic models from measured I-V characteristics curves using a hybrid trust-region reflective algorithm," *Applied Energy*, vol. 232, pp. 36-53, 2018, doi: 10.1016/j.apenergy.2018.09.161.

[31] X. Chen, B. Xu, C. Mei, Y. Ding, K. Li, "Teaching–learning–based artificial bee colony for solar photovoltaic parameter estimation," *Applied Energy*, vol. 212, pp. 1578-1588, 2018, doi: 10.1016/j.apenergy.2017.12.115.

[32] X. Yuan, Y. Xiang, Y. He, "Parameter extraction of solar cell models using mutative-scale parallel chaos optimization algorithm," *Solar Energy*, vol. 108, pp. 238-251, 2014, doi: 10.1016/j.solener.2014.07.013.

[33] D. Alam, D. Yousri, M. Eteiba, "Flower Pollination Algorithm based solar PV parameter estimation," *Energy Conversion and Management*, vol. 101, pp. 410-422, 2015, doi: 10.1016/j.enconman.2015.05.074.

[34] O. Hachana, K. Hemsas, G. Tina, C. Ventura, "Comparison of different metaheuristic algorithms for parameter identification of photovoltaic cell/module," *Journal of Renewable and Sustainable Energy, vol.* 5, p. 053122, 2013, doi: 10.1063/1.4822054.

[35] T. Easwarakhanthan, J. Bottin, I. Bouhouch, C. Boutrit, "Nonlinear sputers," *International Journal of Solar Energy*, vol. 4, pp. 1-12, 1986, doi: 10.1080/01425918608909835.

[36] S. Lidaighbi, M. Elyaqouti, D. Hmamou, D. Saadaoui, K. Assalaou, E. Arjdal, "A new hybrid method to estimate the single-diode model parameters of solar photovoltaic panel," *Energy Conversion and Management: X*, vol. 15, p. 100234, 2022, doi: 10.1016/j.ecmx.2022.100234.

[37] D. Saadaoui, M. Elyaqouti, K. Assalaou, D. Hmamou, S. Lidaighbi, "Parameters optimization of solar PV cell/module using genetic algorithm based on non-uniform mutation," *Energy Conversion and Management: X*, vol. 12, p. 100129, 2021, doi: 10.1016/j.ecmx.2021.100129.

[38] N. Hamid, R. Abounacer, M. Oumhand, M. Feddaoui, D. Agliz, "Parameters identification of photovoltaic solar cells and module using the genetic algorithm with convex combination crossover," *International Journal of Ambient Energy*, vol. 40, no. 5, pp. 517-524, 2018, doi: 10.1080/01430750.2017.1421577.

[39] K. El-Naggar, M. AlRashidi, M. AlHajri, A. Al-Othman, "Simulated Annealing algorithm for photovoltaic parameters identification," *Solar Energy*, vol. 86, no. 1, pp. 266–74, 2012, doi: 10.1016/j.solener.2011.09.032.

[40] H. Mokhliss, A. El-Amiri, K. Rais, "Estimation of five parameters of photovoltaic modules using a synergetic control theory approach," *Journal of Computational Electronics*, vol. 18, pp. 241–250, 2019, doi: 10.1007/s10825-018-1253-2.

[41] N. Tong, W. Pora, "A parameter extraction technique exploiting intrinsic properties of solar cells," *Applied Energy*, vol. 176, pp. 104-115, 2016, doi: 10.1016/j.apenergy.2016.05.064.

[42] M. Naeijian, A. Rahimnejad, S. Ebrahimi, N. Pourmousa, S. Gadsden, "Parameter estimation of PV solar cells and modules using Whippy Harris Hawks Optimization Algorithm," *Energy Reports*, vol. 7, pp. 4047-4063, 2021, doi: 10.1016/j.egyr.2021.06.085.